Relationship of MR imaging of submandibular glands to hyposalivation in Sjogren's syndrome

doi: 10.1111/odi.12941

Original Research

Relationship of MR Imaging of Submandibular Glands to Hyposalivation in Sjögren's Syndrome

Ikuho Kojima, Maya Sakamoto, Masahiro Iikubo, Yusuke Shimada, Takashi Nishioka, Takashi Sasano

Department of Oral Diagnosis, Tohoku University Graduate School of Dentistry

4-1 Seiryo-machi, Aoba-ku, Sendai 980-8575, Japan

Corresponding author:

Ikuho Kojima

Department of Oral Diagnosis

Tohoku University Graduate School of Dentistry

4-1 Seiryo-machi, Aoba-ku, Sendai 980-8575, Japan

Tel: 81-22-717-8390

Fax: 81-22-717-8393

E-mail: ikh-koji213@umin.ac.jp

Running title: MR Imaging and Salivary Flow in Sjögren's Syndrome

Key words: autoimmune disease, salivary glands, Sjögren's syndrome, magnetic resonance imaging

Date of submission: July 10, 2018

Abstract

Objective

We analysed the correlation between magnetic resonance images of the parotid and submandibular glands and the salivary flow rate in patients with Sjögren's syndrome.

Methods

We retrospectively reviewed magnetic resonance images (heterogeneous signal-intensity distribution and gland volume on T1- and fat-suppressed T2-weighted images, and multiple high-signal-intensity spots on magnetic resonance sialograms in the parotid and submandibular glands) obtained from 66 patients who were diagnosed with Sjögren's syndrome. We evaluated the relationship between these imaging features and their salivary flow rates in stimulated and unstimulated conditions.

Results

We found that, as the disease progressed, both the heterogeneous signal-intensity distribution and the volumes of the parotid and the submandibular glands were significantly related to the stimulated and the unstimulated salivary flow rate. These imaging features were more highly correlated in assessments of the submandibular gland than in those of the parotid gland for both stimulated and unstimulated salivary flow rates.

Conclusions

Magnetic resonance image features of heterogeneity and smaller volume in the submandibular gland are reliable for predicting hyposalivation related to the progression of Sjögren's syndrome.

Introduction

Destruction of the acinar tissues of salivary glands in patients with Sjögren's syndrome (SS) result in hyposalivation, i.e., a reduction in salivary flow rate (Bloch et al., 1965; Kohler & Winter, 1985; Manthorpe, 2002). Salivary gland scintigraphy, which is a commonly used diagnostic imaging modality for assessing salivary gland function, has indicated that scintigraphic features correlated well both with the histopathological findings of labial gland biopsies and a reduction in parotid flow rate in SS patients (Daniels et al., 1979). Other researchers using salivary gland scintigraphy have noted that, as the disease progresses, the submandibular gland exhibits greater dysfunction than the parotid gland in SS patients (Umehara et al., 1999; Aung et al., 2000; Tonami et al., 2001; Aksoy et al., 2012). Characteristic magnetic resonance (MR) imaging features of the parotid gland in SS patients include heterogeneous signal-intensity distribution (HD) on T1- and T2-weighted images ("salt and pepper appearance") (Izumi et al., 1996; Vogl et al., 1996) and multiple high-signal-intensity spots (MHS) on MR sialograms ("apple tree appearance") (Ohbayashi et al., 1998; Tonami et al., 1998). The HD represents histopathological destruction of acinar tissue with fat tissue infiltration, while the MHS, which mostly comprised saliva leaked from peripheral ducts, represent ductal abnormalities (Garrett, 1962; Izumi et al., 1997; Niemela et al., 2001). Previous reports also demonstrated that the HD in the parotid gland was related to the salivary flow rate (Izumi et al., 1997), while the MHS were not related to the salivary flow rate on MR sialograms of parotid glands (Niemela et al., 2001). However, these studies did not investigate the submandibular gland. We recently reported that (1) the presence of MHS on MR sialograms and HD on both T1- and fat-suppressed T2-weighted MR images had higher specificity for the submandibular gland than for the parotid gland in patients with SS, and that (2) the submandibular gland volume, but not the volume of parotid or sublingual glands, appeared smaller in SS patients (Kojima et al., 2017). Consequently, we concluded

that such specific changes in the submandibular gland were helpful in assessing SS patients, particularly in advanced cases. Additionally, physiological evidence has shown that more than 65% of unstimulated whole saliva is produced by the submandibular gland, while the parotid gland contributes approximately 20%, despite its massive size (Sreebny, 2010). This background information prompted us to hypothesise that MR imaging of the submandibular gland might closely correlate with hyposalivation as the disease progresses. No studies, however, have focused on the correlation between MR imaging of the submandibular gland and corresponding salivary flow rate in SS patients. We, therefore, retrospectively investigated the relationship between MR imaging of the submandibular gland and the corresponding salivary flow rate in SS patients, in comparison with the parotid gland.

Methods

Our retrospective study was performed in accordance with the Declaration of Helsinki, and was approved by the Institutional Review Board (Tohoku University Graduate School of Dentistry, No. 2017-3-22).

Patients

Sixty-six patients (two males and 64 females; age range, 19–79 years old; mean age, 54 years) with SS participated in this study. Diagnosis of SS was determined by xerostomia as the chief complaint, along with positive anti-SS-A and/or anti-SS-B antibodies in serological tests, and focal lymphocytic sialadenitis in histopathological assessment of labial gland biopsy. A focal score of ≥1 was defined as positive, in accordance with the histopathology criteria of Greenspan et al. (1974). These patients were subsequently definitively diagnosed with SS, in accordance with the criteria proposed by the American College of Rheumatology (Shiboski et al., 2012), as well as the Japanese criteria (Fujibayashi et al., 2004). Human immunodeficiency virus and sarcoidosis were excluded in all patients upon evaluation by autoimmune disease specialists.

Collection of stimulated and unstimulated saliva

Patients were instructed to do nothing to stimulate the flow of saliva for at least 90 min before the collection time. This included tooth brushing, using mouthwash, drinking, chewing, and smoking. Stimulated salivary flow rate was determined using the gum test (Fujibayashi et al., 2004): patients chewed a polyvinyl acetate gum and collected their saliva into a vessel for 10 min. Unstimulated salivary flow rate was tested using the spitting method (Speight et al., 1992; Marton et al., 2008): patients expectorated their saliva for 15 min into a vessel while making as few movements as possible during the procedure. A decrease of salivation was

defined as a flow rate of < 10 mL/10 min for stimulated saliva (Fujibayashi et al., 2004) or < 1.5 mL/15 min (Speight et al., 1992; Marton et al., 2008) for unstimulated saliva.

MR imaging technique

MR examination was performed by a 1.5- or 3.0-Tesla MR imager (Achieva 1.5T or Achieva 3.0T; Royal Philips Electronics, Eindhoven, the Netherlands) with surface coils. We obtained spin-echo transverse T1-weighted images (repetition time/echo time, 477–619/7–12 ms), fast spin-echo transverse fat-suppressed T2-weighted images (repetition time/echo time, 4000–5711/54–90 ms), and high-resolution 3D-MR sialograms (repetition time/echo time/number of signal-intensity acquisitions, 5000/602–675 ms/2), using the same methods (Kojima et al., 2017). T1- and fat-suppressed T2-weighted images were collected using 5-mm section thickness with a 1 mm intersection gap, acquisition matrix of 512 × 358, and FOV of 210 mm. Three-dimensional MR sialograms comprised 1 mm with a gapless acquisition, acquisition matrix of 512 × 512, and FOV of 200 mm, and used a heavily T2-weighted fast spin-echo sequence, based on a previous report. This 3D technique of the MR sialogram has been excellent for detecting fine salivary gland ducts and small abnormalities (Sakamoto et al., 2001). The MR sialograms consisted of 20-slice images.

MR Imaging analysis

We exported all MR images as Digital Imaging and Communications in Medicine (DICOM) files and imported them into specially designed DICOM viewing software (Aquarius NET; TeraRecon, Foster City, CA, USA); all MR images were separated from clinical information. Two board-certified oral and maxillofacial radiologists (I.K. and M.S., with 13 and 33 years of experience, respectively) independently reviewed random-ordered MR images under the condition that they could not know any clinical information except that the MR images were

obtained from patients with a definite diagnosis of SS, on the basis of the criteria described in the "Patients" subsection (above). The reviewers evaluated (i) HD on T1- and fat-suppressed T2-weighted images, (ii) MHS on MR sialograms and (iii) the volumes of each respective major salivary gland. We estimated the parotid and submandibular glands, but not the sublingual gland, in the present study, because the sublingual gland has demonstrated low diagnostic value in diagnosing SS on MR imaging (Kojima et al., 2017). (i) We graded the HD depending on the degree of the acinar tissue destruction with fat tissue infiltration, which was previously reported to demonstrate a heterogeneous distribution of very high signal-intensity on T1-weighted images and very low signal-intensity on fat-suppressed T2-weighed images (Izumi et al., 1996; Izumi et al., 1997). We excluded microcysts, observed as high-signal-intensity spots on fat-suppressed T2-weighted images, from the HD grading, as microcysts are closely related to the MHS. HD was assessed as grade 0 (definitely normal: homogeneous), 1 (probably normal: almost homogeneous), 2 (probably abnormal: slightly heterogeneous), 3 (clearly abnormal: moderately heterogeneous), and 4 (definitely abnormal: severely heterogeneous) by the objective evaluation of the radiologists (**Figure 1**). We assessed severely atrophied glands which had almost been displaced by fat tissue as grade 4 (severe heterogeneous). (ii) By using X-ray sialography criteria established in previous reports, we graded the MHS on the basis of the size of the high-signal-intensity spots, which were composed of saliva leaked from peripheral ducts (Niemela et al., 2001). MHS was assessed as stage 0 (no cavities found), 1 (cavities $\leq$ 1 mm in diameter), 2 (cavities 1–2 mm in diameter), 3 (cavities > 2 mm in diameter), and 4 (severe irregular dilatation of the main duct with bizarrely patterned cavities). (iii) The volume of the salivary glands was measured, as previously reported (Ono et al., 2006; Kojima et al., 2017). The parotid and submandibular gland volumes were calculated as the sum of all transverse section areas, multiplied by section thickness. Reviewers resolved disagreements of grading and staging by discussion.

Statistical analysis

The relationships between the HD grade or MHS stage and the salivary flow rate were analysed using the Kruskal-Wallis rank sum test. For multiple comparisons, the Steel-Dwass method was used in further investigation. Correlations between the salivary gland volume and the salivary flow rate were tested by Spearman's rank correlation coefficient (ρ). The strength of correlation was classified as negligible or no correlation ($|\rho| \leq 0.20$), weak ($|\rho| = 0.21$ to 0.40), moderate ($|\rho| = 0.41$ to 0.70), or strong ($|\rho| = 0.71$ to 1.00). We analysed diagnostic performance and cut-off values for diagnosing hyposalivation by using receiver operating characteristic (ROC) curve analysis. Diagnostic performance was evaluated between the parotid and submandibular glands by comparing sensitivity, specificity, area under the ROC curve (AUC) and its 95% confidence interval (95%CI). *P*-values of < 0.05 were defined as significantly different. We measured kappa coefficient (ƙ) of interobserver agreement between the two reviewers for grading and staging in the imaging analysis. The ƙ value of 0.01 to 0.20 indicated slight; 0.21 to 0.40, fair; 0.41 to 0.60, moderate; 0.61 to 0.80, substantial; 0.81 to 1.00, excellent agreement. For statistical analysis, we used EZR software (Saitama Medical Center, Jichi Medical University), which provides a graphical interface for R (version 2.13.0; The R Foundation for Statistical Computing, Vienna, Austria).

Results

Salivary flow rate

Forty-two of the 66 patients with SS (63.6%) showed decreased salivation in the stimulated salivary flow rate test (< 10 mL/10 min) and 44 (66.7%) showed a decreased unstimulated salivary flow rate (< 1.5 mL/15 min) (**Table**). There were no significant differences in the percentage of decreased salivation between stimulated and unstimulated conditions.

Relationship between MR imaging and salivary flow rate

HD grade on MR imaging (**Figure 1**) was significantly related to both stimulated and unstimulated salivary flow rates in parotid and submandibular glands: advanced grades corresponded to a greater reduction in salivary flow (**Figure 2A, 2B, 2E, 2F**). However, there was no significant relationship between the MHS stage and the salivary flow rate in either the parotid or the submandibular glands in both stimulated and unstimulated conditions (**Figure 2C, 2D, 2G, 2H**).

The AUC for the HD grade was significantly greater in the submandibular gland than in the parotid gland both for stimulated (parotid gland: AUC 0.786, 95%CI 0.682–0.889, vs. submandibular gland: AUC 0.898, 95%CI 0.827–0.969; $P < 0.05$, **Figure 3A**) and for unstimulated (parotid gland: AUC 0.675, 95%CI 0.549–0.8, vs. submandibular gland: AUC 0.813, 95%CI 0.712–0.913; $P < 0.01$, **Figure 3B**) salivary flow rates. The best cut-off values of the HD grade that showed the highest diagnostic accuracy were grade 3 in the parotid gland (stimulated salivary flow rate: sensitivity 0.548, specificity 0.958; unstimulated salivary flow rate: sensitivity 0.5, specificity 0.909) and grade 2 in the submandibular gland (stimulated salivary flow rate: sensitivity 0.81, specificity 0.875; unstimulated salivary flow rate: sensitivity 0.727, specificity 0.773).

Correlation between salivary gland volume and salivary flow rate

The respective volumes of the parotid and submandibular glands were significantly correlated both with the stimulated (ρ = 0.32 and 0.57) (**Figure 4A, 4B**) and the unstimulated salivary flow rates (ρ = 0.40 and 0.63) (**Figure 4C, 4D**). These ρ values exhibited a weak correlation in the parotid gland, but a moderate correlation in the submandibular gland.

The AUC for the gland volume was significantly greater in the submandibular gland than in the parotid gland both for the stimulated (parotid gland: AUC 0.653, 95%CI 0.518–0.788, vs. submandibular gland: AUC 0.861, 95%CI 0.766–0.956; $P < 0.001$, **Figure 5A**) and for unstimulated (parotid gland: AUC 0.645, 95%CI 0.514–0.777, vs. submandibular gland: AUC 0.805, 95%CI 0.699–0.911; $P < 0.05$, **Figure 5B**) salivary flow rates. The best cut-off values of the parotid gland volume that showed the highest diagnostic accuracy were 35.7 cm^3 for stimulated (sensitivity 0.667, specificity 0.583) and 27.7 cm^3 for unstimulated (sensitivity 0.364, specificity 0.955) salivary flow rate. The best cut-off values of submandibular gland volume were 8.03 cm^3 for stimulated (sensitivity 0.905, specificity 0.708) and 4.64 cm^3 for unstimulated (sensitivity 0.591, specificity 0.955) salivary flow rate.

Interobserver agreement

The respective kappa values of the HD analysis for the parotid and submandibular glands were 0.83 and 0.78. The respective kappa values of the MHS analysis for the parotid and submandibular glands were 0.89 and 0.92. The strength of agreement was substantial for HD in submandibular glands, excellent for HD in parotid gland, and excellent for MHS in both parotid and submandibular glands.

Discussion

1 Relationship between MR imaging and salivary flow rate in patients with SS

Many patients with SS suffer from xerostomia and a subjective feeling of oral dryness because this condition can affect speech, mastication, swallowing, taste acuity, and ultimately the quality of life (Sreebny, 2010), based on a severe decrease in salivary flow rate. Histopathological features of the disease include lymphocytic infiltration, fat tissue infiltration, and destruction of the acinar tissues, which result in the atrophy of salivary glands (Bloch et al., 1965; Kohler & Winter, 1985; Manthorpe, 2002). Labial gland biopsy features have been shown to correlate closely with hyposalivation as the disease progresses (Chisholm & Mason, 1968; Daniels et al., 1979; Daniels, 1984).

To assess the pathological progression in salivary glands on MR images, we studied the HD grade on T1- and fat-suppressed T2-weighted images, as well as the MHS stage on MR sialograms, based on prior reports (Izumi et al., 1996; Izumi et al., 1997). We demonstrated that the HD grade is significantly related to the salivary flow rate under both stimulated and unstimulated conditions, in both parotid and submandibular glands in SS patients (**Figure 2A, 2B, 2E, 2F**); however, there was no significant relationship between the MHS stage and stimulated or unstimulated salivary flow rate in either the parotid or submandibular glands (**Figure 2C, 2D, 2G, 2H**). Previous studies found that HD in the parotid gland represents histopathological destruction of the acinar tissue and fat tissue infiltration, while MHS represents ductal abnormalities (Garrett, 1962; Izumi et al., 1997; Niemela et al., 2001). Therefore, HD is considered to be more strongly and directly related to the salivary flow rate than MHS, because acinar tissue produces the saliva. Additionally, it has been reported that (1) diffusely scattered fat deposition in the parotid gland on MR imaging is a characteristic feature in SS patients, but is not present in inflamed parotid glands (Izumi et al., 1996); (2) the severity of destruction and fat deposition in SS patients' parotid

glands is associated with the stimulated salivary flow rate using MR imaging and CT (Izumi et al., 1997); and (3) the severity of abnormalities on the MR sialogram in SS patients' parotid glands is not associated with the unstimulated salivary flow rate (Niemela et al., 2001). These reports corroborate our findings that HD in the salivary gland is strongly related to the salivary flow rate in accordance with the progress of the disease.

2 Correlation between MR imaging and salivary flow rate in patients with SS: Submandibular vs parotid gland

2-1 HD in MR imaging in submandibular vs parotid glands

Few studies using MR images to date have focused on changes of the submandibular gland with respect to the progress of SS. We recently reported that HD on T1- and fat-suppressed T2-weighted MR images has higher specificity in the submandibular gland than in the parotid gland in SS patients (Kojima et al., 2017). Consequently, we have deduced that such specific changes of the submandibular gland would aid in assessment of SS patients, particularly in advanced cases. In the current study, we focused on the relationship between MR imaging of the submandibular gland and the salivary flow rate, in comparison with the parotid gland. We excluded the sublingual gland in this study because of its low diagnostic value based on its smaller volume, greater individual or age differences in the size, and low interobserver agreement of the imaging analysis, when compared with the parotid and submandibular glands (Sumi et al., 1999; Kojima et al., 2017). To compare the two salivary glands and to analyse which imaging features were superior for evaluating decreases in the salivary flow rate, we used ROC curve analysis which allows comparison of the diagnostic performance in a multiple examinations (Griner et al., 1981). Using this method, we have demonstrated that HD is more sensitive in the submandibular gland than in the parotid gland with respect to hyposalivation, both in stimulated and unstimulated conditions in SS patients

(**Figure 3A, 3B**). The reason that HD was more closely related with salivary flow rate in the submandibular gland, compared with the parotid gland, could be attributed to two factors. The first factor relates to a physiological aspect. Spontaneous salivary flow derived mainly from the submandibular gland, and less often from the parotid gland in the unstimulated condition (Aung et al., 2001), *i.e.*, more than 65% of unstimulated saliva is secreted by the submandibular gland (Sreebny, 2010). These reports are consistent with our findings. The second factor is a pathological aspect. It has been demonstrated that the submandibular gland is further impaired than the parotid gland upon evaluation of scintigraphic parameters in SS patients, which is accompanied by hyposalivation in the unstimulated condition (Dugonjic et al., 2014). Many studies using salivary scintigraphy under lemon stimulation condition also demonstrated that the function of the submandibular gland was more impaired than that of the parotid gland in SS patients (Umehara et al., 1999; Aung et al., 2000; Tonami et al., 2001; Aksoy et al., 2012). Aung et al. and Umehara et al. indicated that tracer accumulation decreased more in the submandibular gland, compared with the parotid gland, in SS patients (Umehara et al., 1999; Aung et al., 2000). Additionally, Tonami et al. and Aksoy et al., using salivary scintigraphy, concluded that the submandibular gland became more impaired than the parotid gland with disease progression (Tonami et al., 2001; Aksoy et al., 2012). These scintigraphy findings prompt the conclusion that MR imaging can more accurately depict a decrease in the salivary flow rate in the submandibular gland, compared with the parotid gland, both for unstimulated and stimulated conditions in SS patients.

2-2 Changes in volume on MR imaging in submandibular vs parotid glands

This study has shown that the parotid and the submandibular glands volume is significantly correlated with the stimulated and unstimulated salivary flow rates (**Figure 4A-D**) in SS patients. Characteristic MR imaging features in SS patients are atrophy and

swelling of the salivary glands, and HD and MHS (Vogl et al., 1996). Swelling of the glands is caused by autoimmune inflammation, and shrunken glands are frequently observed on MR images as a result of severe atrophic change caused by continuous chronic inflammation (**Figure 1**). The parotid and submandibular gland volume correlates with the stimulated and unstimulated salivary flow rate in healthy humans (Ericson et al., 1972; Dawes et al., 1978; Ono et al., 2006). Taking these reports into account, it is reasonable to assume that the acinar tissue volume observed on MR imaging correlates with the salivary flow rate. We also demonstrated that the submandibular gland volume measured on MR imaging was more significantly correlated with the stimulated and unstimulated salivary flow rate than the parotid gland volume, as compared by ROC curve analysis (**Figure 5A, 5B**). MR images have shown that the parotid gland in SS patients reveals atrophy and swelling, whereas in the submandibular gland, atrophy is the dominant feature, rather than swelling (Vogl et al., 1996; Kojima et al., 2017). Taken together, we believe that our results indicate that a smaller submandibular gland volume is an aid in predicting hyposalivation in patients with SS as the disease progresses.

3 Limitations of the study and future research

We have demonstrated that MR imaging of HD and the volume of the submandibular gland can predict a decrease in the salivary flow rate, which is a distressing symptom for patients with SS. To clarify the precise relationship between MR imaging and the progression of the disease, histopathological evaluation including the measurement of acinar tissue and fat deposition should be undertaken by salivary gland biopsy. Histopathological and molecular studies are also needed to clarify the mechanism by which the submandibular glands are more severely impaired.

Conclusions

We have demonstrated by MR imaging that heterogeneity and a smaller volume of the submandibular gland are reliable features for predicting hyposalivation associated with progression of SS in patients with the disease.

Acknowledgements

This study was supported by JSPS Grants-in-Aid for Scientific Research (Grant Number 15K11287). We thank Helen Jeays, BDSc AE, and Ryan Chastain-Gross, PhD, from Edanz Group (www.edanzediting.com/ac) for editing a draft of this manuscript.

Conflicts of interest: none to declare.

References

Aksoy T, Kiratli PO and Erbas B (2012). Correlations between histopathologic and scintigraphic parameters of salivary glands in patients with Sjögren's syndrome. *Clinical rheumatology* **31**: 1365-70.

Aung W, Murata Y, Ishida R, Takahashi Y, Okada N and Shibuya H (2001). Study of quantitative oral radioactivity in salivary gland scintigraphy and determination of the clinical stage of Sjögren's syndrome. *J Nucl Med* **42**: 38-43.

Aung W, Yamada I, Umehara I, Ohbayashi N, Yoshino N and Shibuya H (2000). Sjögren's syndrome: comparison of assessments with quantitative salivary gland scintigraphy and contrast sialography. *J Nucl Med* **41**: 257-62.

Bloch KJ, Buchanan WW, Wohl MJ and Bunim JJ (1965). Sjögren's Syndrome. A Clinical, Pathological, and Serological Study of Sixty-Two Cases. A Clinical, Pathological, and Serological Study of Sixty-Two Cases. *Medicine (Baltimore)* **44**: 187-231.

Chisholm DM and Mason DK (1968). Labial salivary gland biopsy in Sjögren's disease. *J Clin Pathol* **21**: 656-60.

Daniels TE (1984). Labial salivary gland biopsy in Sjögren's syndrome. Assessment as a diagnostic criterion in 362 suspected cases. *Arthritis and rheumatism* **27**: 147-56.

Daniels TE, Powell MR, Sylvester RA and Talal N (1979). An evaluation of salivary scintigraphy in Sjögren's syndrome. *Arthritis and rheumatism* **22**: 809-14.

Dawes C, Cross HG, Baker CG and Chebib FS (1978). The influence of gland size on the flow rate and composition of human parotid saliva. *Dent J* **44**: 21-5.

Dugonjic S, Stefanovic D, Ethurovic B, Spasic-Jokic V and Ajdinovic B (2014). Evaluation of diagnostic parameters from parotid and submandibular dynamic salivary glands scintigraphy and unstimulated sialometry in Sjögren's syndrome. *Hell J Nucl Med* **17**: 116-22.

Ericson S, Hedin M and Wiberg A (1972). Variability of the submandibular flow rate in man with special reference to the size of the gland. *Odontol Revy* **23**: 411-20.

Fujibayashi T, Sugai S, Miyasaka N, Hayashi Y and Tsubota K (2004). Revised Japanese criteria for Sjögren's syndrome (1999): availability and validity. *Modern rheumatology / the Japan Rheumatism Association* **14**: 425-34.

Garrett JR (1962). Some Observations on Human Submandibular Salivary Glands. *Proc R Soc Med* **55**: 488-91.

Greenspan JS, Daniels TE, Talal N and Sylvester RA (1974). The histopathology of Sjögren's syndrome in labial salivary gland biopsies. *Oral Surg Oral Med Oral Pathol* **37**: 217-29.

Griner PF, Mayewski RJ, Mushlin AI and Greenland P (1981). Selection and interpretation of diagnostic tests and procedures. Principles and applications. *Ann Intern Med* **94**: 557-92.

Izumi M, Eguchi K, Nakamura H, Nagataki S and Nakamura T (1997). Premature fat deposition in the salivary glands associated with Sjögren's syndrome: MR and CT evidence. *AJNR. American journal of neuroradiology* **18**: 951-8.

Izumi M, Eguchi K, Ohki M, Uetani M, Hayashi K, Kita M, Nagataki S and Nakamura T (1996). MR imaging of the parotid gland in Sjögren's syndrome: a proposal for new diagnostic criteria. *AJR. American journal of roentgenology* **166**: 1483-7.

Kohler PF and Winter ME (1985). A quantitative test for xerostomia. The Saxon test, an oral equivalent of the Schirmer test. *Arthritis and rheumatism* **28**: 1128-32.

Kojima I, Sakamoto M, Iikubo M, Kumamoto H, Muroi A, Sugawara Y, Satoh-Kuriwada S and Sasano T (2017). Diagnostic performance of MR imaging of three major salivary glands for Sjögren's syndrome. *Oral diseases* **23**: 84-90.

Manthorpe R (2002). Sjögren's syndrome criteria. *Annals of the rheumatic diseases* **61**: 482-4.

Marton K, Madlena M, Banoczy J, Varga G, Fejerdy P, Sreebny LM and Nagy G (2008). Unstimulated whole saliva flow rate in relation to sicca symptoms in Hungary. *Oral diseases* **14**: 472-7.

Niemela RK, Paakko E, Suramo I, Takalo R and Hakala M (2001). Magnetic resonance imaging and magnetic resonance sialography of parotid glands in primary Sjögren's syndrome. *Arthritis and rheumatism* **45**: 512-8.

Ohbayashi N, Yamada I, Yoshino N and Sasaki T (1998). Sjögren syndrome: comparison of assessments with MR sialography and conventional sialography. *Radiology* **209**: 683-8.

Ono K, Morimoto Y, Inoue H, Masuda W, Tanaka T and Inenaga K (2006). Relationship of the

unstimulated whole saliva flow rate and salivary gland size estimated by magnetic resonance image in healthy young humans. *Arch Oral Biol* **51**: 345-9.

Sakamoto M, Sasano T, Higano S, Takahashi S, Nagasaka T, Yanagawa I, Hosogai Y, Tamura H, Iikubo M and Shoji N (2001). Evaluation of pulse sequences used for magnetic resonance sialography. *Dento maxillo facial radiology* **30**: 276-84.

Shiboski SC, Shiboski CH, Criswell L, Baer A, Challacombe S, Lanfranchi H, Schiodt M, Umehara H, Vivino F, Zhao Y, Dong Y, Greenspan D, Heidenreich AM, Helin P, Kirkham B, Kitagawa K, Larkin G, Li M, Lietman T, Lindegaard J, McNamara N, Sack K, Shirlaw P, Sugai S, Vollenweider C, Whitcher J, Wu A, Zhang S, Zhang W, Greenspan J and Daniels T (2012). American College of Rheumatology classification criteria for Sjögren's syndrome: a data-driven, expert consensus approach in the Sjogren's International Collaborative Clinical Alliance cohort. *Arthritis care & research* **64**: 475-87.

Speight PM, Kaul A and Melsom RD (1992). Measurement of whole unstimulated salivary flow in the diagnosis of Sjögren's syndrome. *Annals of the rheumatic diseases* **51**: 499-502.

Sreebny L (2010). *The odd couple: dry mouth and salivary flow,* Wiley-Blackwell: Iowa.

Sumi M, Izumi M, Yonetsu K and Nakamura T (1999). Sublingual gland: MR features of normal and diseased states. *AJR. American journal of roentgenology* **172**: 717-22.

Tonami H, Higashi K, Matoba M, Yokota H, Yamamoto I and Sugai S (2001). A comparative study between MR sialography and salivary gland scintigraphy in the diagnosis of Sjögren's syndrome. *Journal of computer assisted tomography* **25**: 262-8.

Tonami H, Ogawa Y, Matoba M, Kuginuki Y, Yokota H, Higashi K, Okimura K, Yamamoto I and Sugai S (1998). MR sialography in patients with Sjögren syndrome. *AJNR. American journal of neuroradiology* **19**: 1199-203.

Umehara I, Yamada I, Murata Y, Takahashi Y, Okada N and Shibuya H (1999). Quantitative evaluation of salivary gland scintigraphy in Sjögren's syndrome. *J Nucl Med* **40**: 64-9.

Vogl TJ, Dresel SH, Grevers G, Spath M, Bergman C, Balzer J and Lissner J (1996). Sjögren's syndrome: MR imaging of the parotid gland. *European radiology* **6**: 46-51.

Figure Legends

Figure 1. Grade of heterogeneous signal-intensity distribution on T1- and fat-suppressed T2-weighted images in the parotid and submandibular glands. Grade 0 (definitely normal: homogeneous), Grade 1 (probably normal: almost homogeneous), Grade 2 (probably abnormal: slight heterogeneous), Grade 3 (clearly abnormal: moderate heterogeneous), Grade 4 (definitely abnormal: severe heterogeneous). As the grade advances, the area of acinar tissue destruction with fat tissue infiltration expands in the parotid or submandibular gland: fat infiltration is observed as a very high signal-intensity area on T1-weighted images and as a very low signal-intensity area on fat-suppressed T2-weighed images. Severely atrophied submandibular gland (arrow heads) and parotid gland (almost displaced by fat tissue) were assessed as grade 4.

Figure 2. Relationship between MR imaging and salivary flow rate. The HD grade vs the stimulated salivary flow rate in the parotid (A) and submandibular (B) glands. The MHS stage vs the stimulated salivary flow rate in the parotid (C) and submandibular (D) glands. The HD grade vs the unstimulated salivary flow rate in the parotid (E) and submandibular (F) glands. The MHS stage vs the unstimulated salivary flow rate in the parotid (G) and submandibular (H) glands. HD = heterogeneous signal-intensity distribution; MHS = multiple high signal-intensity spots. Kruskal-Wallis rank sum test and Steel-Dwass method: * $P < 0.05$, ** $P < 0.01$, *** $P < 0.001$.

Figure 3. ROC curve analysis of HD between the parotid and submandibular glands, for the stimulated (A) and unstimulated (B) salivary flow rate. Black and white points show cut-off points. HD = heterogeneous signal-intensity distribution; PG = parotid gland; SMG = submandibular gland; ROC = receiver operating characteristic. Difference in the area under the ROC curve between the parotid and the submandibular glands: * $P < 0.05$, **

$P < 0.01$.

Figure 4. Correlation between salivary gland volume and salivary flow rate. The correlation between the parotid gland volume and the stimulated salivary flow rate (A), the submandibular gland volume and the stimulated salivary flow rate (B), the parotid gland volume and the unstimulated salivary flow rate (C), and the submandibular gland volume and the unstimulated salivary flow rate (D). Spearman's rank correlation coefficient (ρ) test: ** $P < 0.01$, *** $P < 0.001$.

Figure 5. ROC curve analysis of salivary gland volume between the parotid and submandibular glands for the stimulated (A) and unstimulated (B) salivary flow rate. Black and white points show cut-off points. PG = parotid gland; SMG = submandibular gland; ROC = receiver operating characteristic. Difference in the area under the ROC curve between the parotid and submandibular glands: * $P < 0.05$, *** $P < 0.001$.

Table. Salivary flow rate and MR imaging

	Stimulated salivary flow rate (cut off: 10 mL/10 min)	Unstimulated salivary flow rate (cut off: 1.5 mL/15 min)
Normal	24	22
Abnormal (hyposalivation)	42	44

	HD in PG	HD in SMG	MHS in PG	MHS in SMG
Grade/Stage 0	7	21	23	54
Grade/Stage 1	15	8	15	7
Grade/Stage 2	20	17	21	3
Grade/Stage 3	17	11	7	2
Grade/Stage 4	7	9	0	0

HD = heterogeneous signal-intensity distribution; MHS = multiple high signal-intensity spots; PG = parotid gland; SMG = submandibular gland.

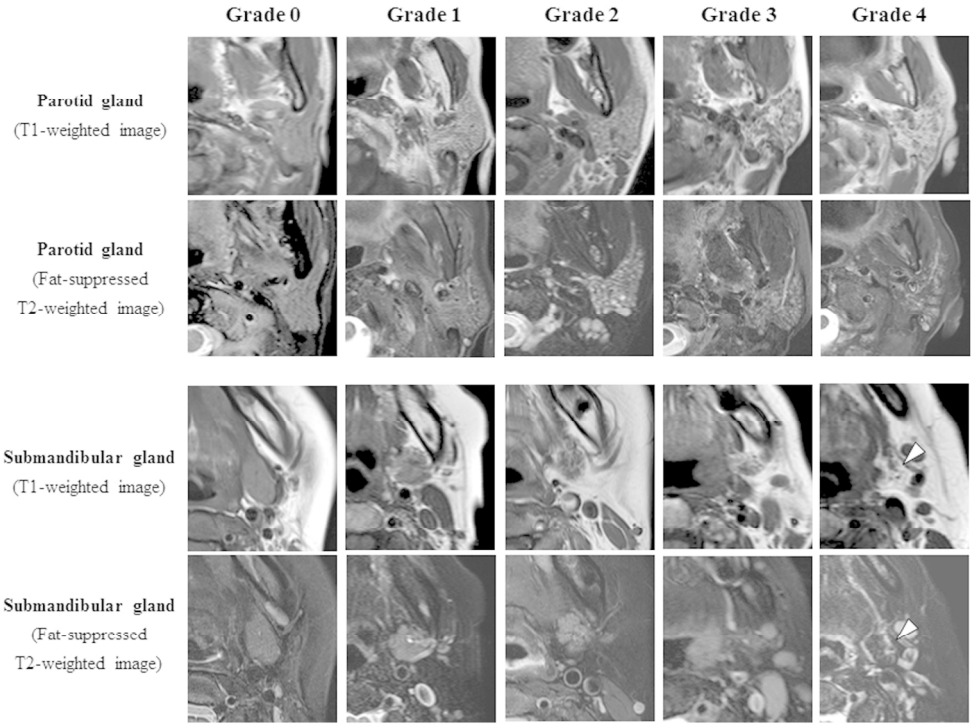

Figure 1. Grade of heterogeneous signal-intensity distribution on T1- and fat-suppressed T2-weighted images in the parotid and submandibular glands. Grade 0 (definitely normal: homogeneous), Grade 1 (probably normal: almost homogeneous), Grade 2 (probably abnormal: slight heterogeneous), Grade 3 (clearly abnormal: moderate heterogeneous), Grade 4 (definitely abnormal: severe heterogeneous). As the grade advances, the area of acinar tissue destruction with fat tissue infiltration expands in the parotid or submandibular gland: fat infiltration is observed as a very high signal-intensity area on T1-weighted images and as a very low signal-intensity area on fat-suppressed T2-weighed images. Severely atrophied submandibular gland (arrow heads) and parotid gland (almost displaced by fat tissue) were assessed as grade 4.

152x114mm (300 x 300 DPI)

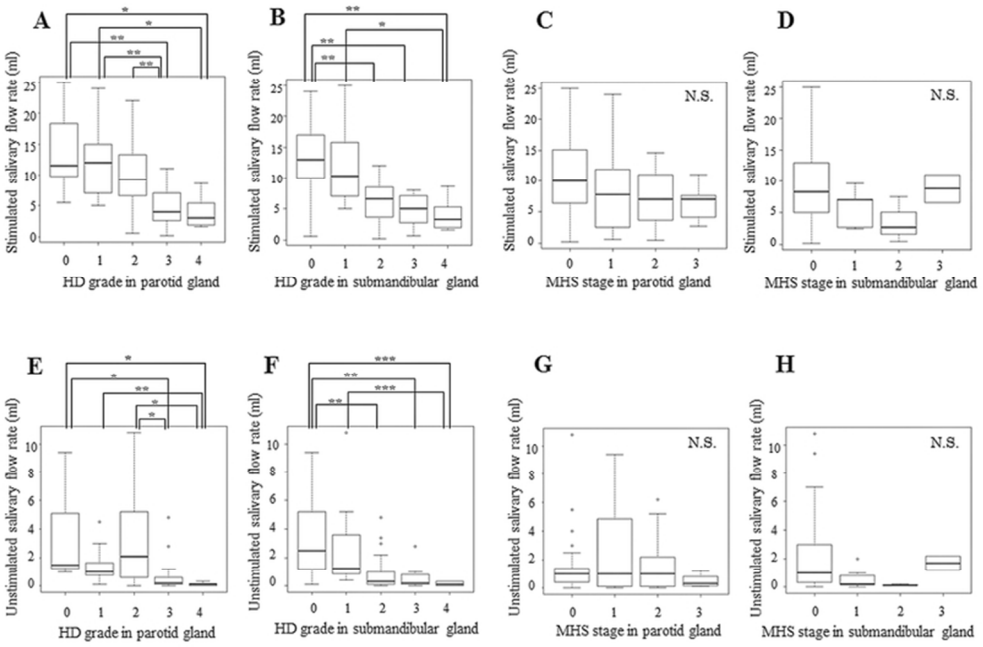

Figure 2. Relationship between MR imaging and salivary flow rate. The HD grade vs the stimulated salivary flow rate in the parotid (A) and submandibular (B) glands. The MHS stage vs the stimulated salivary flow rate in the parotid (C) and submandibular (D) glands. The HD grade vs the unstimulated salivary flow rate in the parotid (E) and submandibular (F) glands. The MHS stage vs the unstimulated salivary flow rate in the parotid (G) and submandibular (H) glands. HD = heterogeneous signal-intensity distribution; MHS = multiple high signal-intensity spots. Kruskal-Wallis rank sum test and Steel-Dwass method: * $P < 0.05$, ** $P < 0.01$, *** $P < 0.001$.

69x47mm (300 x 300 DPI)

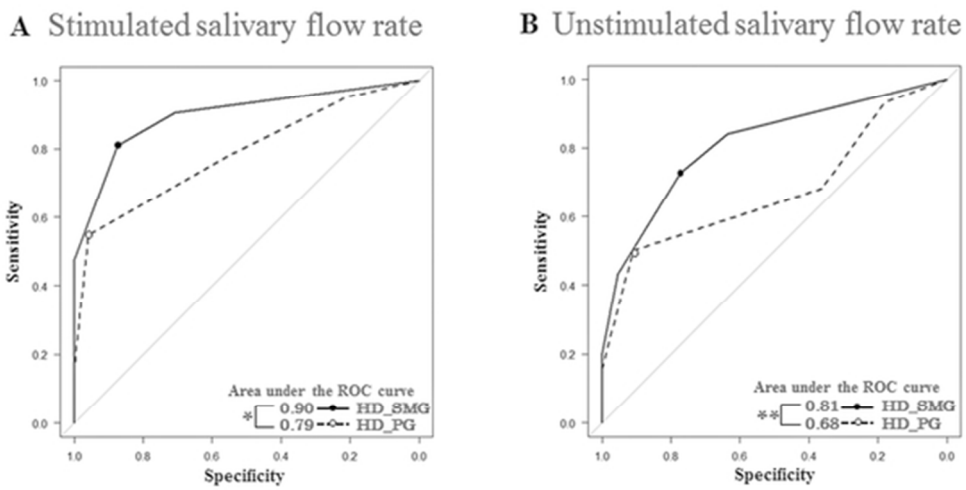

Figure 3. ROC curve analysis of HD between the parotid and submandibular glands, for the stimulated (A) and unstimulated (B) salivary flow rate. Black and white points show cut-off points. HD = heterogeneous signal-intensity distribution; PG = parotid gland; SMG = submandibular gland; ROC = receiver operating characteristic. Difference in the area under the ROC curve between the parotid and the submandibular glands: * $P < 0.05$, ** $P < 0.01$.

52x27mm (300 x 300 DPI)

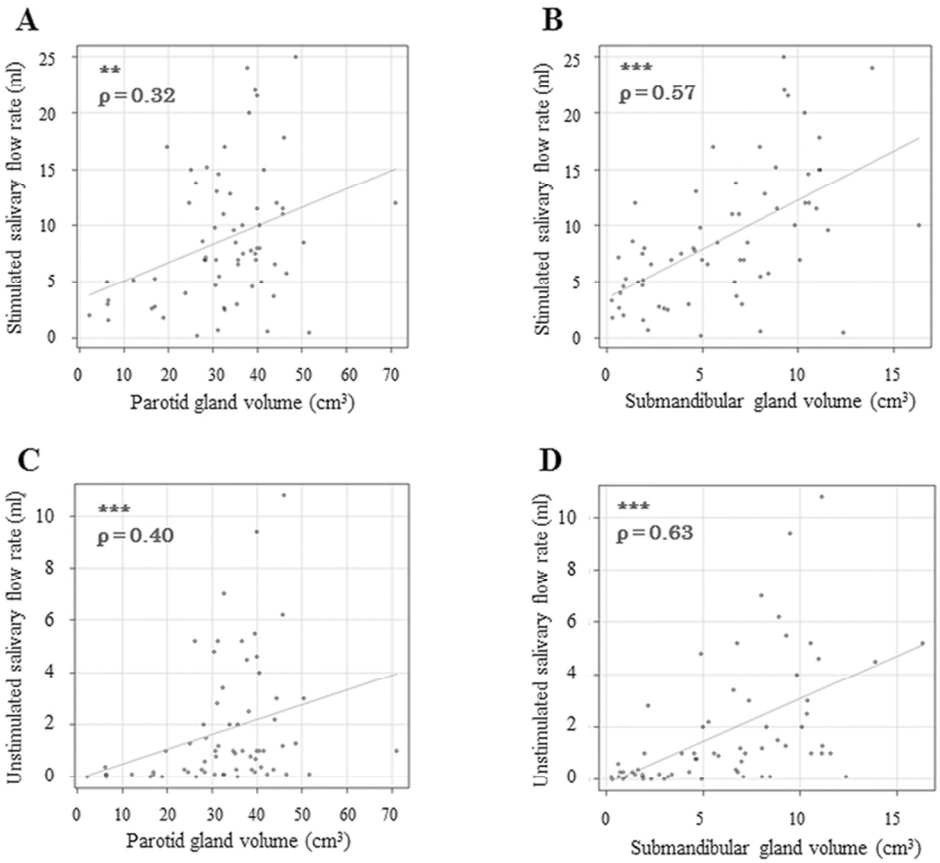

Figure 4. Correlation between salivary gland volume and salivary flow rate. The correlation between the parotid gland volume and the stimulated salivary flow rate (A), the submandibular gland volume and the stimulated salivary flow rate (B), the parotid gland volume and the unstimulated salivary flow rate (C), and the submandibular gland volume and the unstimulated salivary flow rate (D). Spearman's rank correlation coefficient (ρ) test: ** $P < 0.01$, *** $P < 0.001$.

76x67mm (300 x 300 DPI)

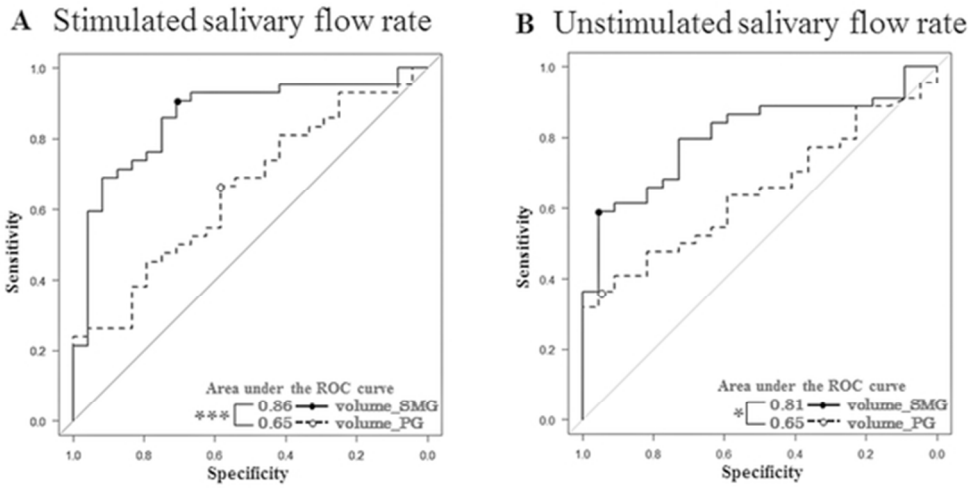

Figure 5. ROC curve analysis of salivary gland volume between the parotid and submandibular glands for the stimulated (A) and unstimulated (B) salivary flow rate. Black and white points show cut-off points. PG = parotid gland; SMG = submandibular gland; ROC = receiver operating characteristic. Difference in the area under the ROC curve between the parotid and submandibular glands: * $P < 0.05$, *** $P < 0.001$.

53x28mm (300 x 300 DPI)

STROBE Statement—checklist of items that should be included in reports of observational studies

	Item No	Recommendation
Title and abstract	1	(*a*) Indicate the study's design with a commonly used term in the title or the abstract
		(*b*) Provide in the abstract an informative and balanced summary of what was done and what was found
Introduction		
Background/rationale	2	Explain the scientific background and rationale for the investigation being reported
Objectives	3	State specific objectives, including any prespecified hypotheses
Methods		
Study design	4	Present key elements of study design early in the paper
Setting	5	Describe the setting, locations, and relevant dates, including periods of recruitment, exposure, follow-up, and data collection
Participants	6	(*a*) *Cohort study*—Give the eligibility criteria, and the sources and methods of selection of participants. Describe methods of follow-up *Case-control study*—Give the eligibility criteria, and the sources and methods of case ascertainment and control selection. Give the rationale for the choice of cases and controls *Cross-sectional study*—Give the eligibility criteria, and the sources and methods of selection of participants
		(*b*) *Cohort study*—For matched studies, give matching criteria and number of exposed and unexposed *Case-control study*—For matched studies, give matching criteria and the number of controls per case
Variables	7	Clearly define all outcomes, exposures, predictors, potential confounders, and effect modifiers. Give diagnostic criteria, if applicable
Data sources/ measurement	8*	For each variable of interest, give sources of data and details of methods of assessment (measurement). Describe comparability of assessment methods if there is more than one group
Bias	9	Describe any efforts to address potential sources of bias
Study size	10	Explain how the study size was arrived at
Quantitative variables	11	Explain how quantitative variables were handled in the analyses. If applicable, describe which groupings were chosen and why
Statistical methods	12	(*a*) Describe all statistical methods, including those used to control for confounding
		(*b*) Describe any methods used to examine subgroups and interactions
		(*c*) Explain how missing data were addressed
		(*d*) *Cohort study*—If applicable, explain how loss to follow-up was addressed *Case-control study*—If applicable, explain how matching of cases and controls was addressed *Cross-sectional study*—If applicable, describe analytical methods taking account of sampling strategy
		(*e*) Describe any sensitivity analyses

Continued on next page

Results		
Participants	13*	(a) Report numbers of individuals at each stage of study—eg numbers potentially eligible, examined for eligibility, confirmed eligible, included in the study, completing follow-up, and analysed
		(b) Give reasons for non-participation at each stage
		(c) Consider use of a flow diagram
Descriptive data	14*	(a) Give characteristics of study participants (eg demographic, clinical, social) and information on exposures and potential confounders
		(b) Indicate number of participants with missing data for each variable of interest
		(c) *Cohort study*—Summarise follow-up time (eg, average and total amount)
Outcome data	15*	*Cohort study*—Report numbers of outcome events or summary measures over time
		Case-control study—Report numbers in each exposure category, or summary measures of exposure
		Cross-sectional study—Report numbers of outcome events or summary measures
Main results	16	(*a*) Give unadjusted estimates and, if applicable, confounder-adjusted estimates and their precision (eg, 95% confidence interval). Make clear which confounders were adjusted for and why they were included
		(*b*) Report category boundaries when continuous variables were categorized
		(*c*) If relevant, consider translating estimates of relative risk into absolute risk for a meaningful time period
Other analyses	17	Report other analyses done—eg analyses of subgroups and interactions, and sensitivity analyses
Discussion		
Key results	18	Summarise key results with reference to study objectives
Limitations	19	Discuss limitations of the study, taking into account sources of potential bias or imprecision. Discuss both direction and magnitude of any potential bias
Interpretation	20	Give a cautious overall interpretation of results considering objectives, limitations, multiplicity of analyses, results from similar studies, and other relevant evidence
Generalisability	21	Discuss the generalisability (external validity) of the study results
Other information		
Funding	22	Give the source of funding and the role of the funders for the present study and, if applicable, for the original study on which the present article is based

*Give information separately for cases and controls in case-control studies and, if applicable, for exposed and unexposed groups in cohort and cross-sectional studies.

Note: An Explanation and Elaboration article discusses each checklist item and gives methodological background and published examples of transparent reporting. The STROBE checklist is best used in conjunction with this article (freely available on the Web sites of PLoS Medicine at http://www.plosmedicine.org/, Annals of Internal Medicine at http://www.annals.org/, and Epidemiology at http://www.epidem.com/). Information on the STROBE Initiative is available at www.strobe-statement.org.